Fabrication and Testing of a Bi-2223 Test Coil for High Field NMR Magnets

William Scott Marshall, Mark D. Bird, David C. Larbalestier, Dustin M. McRae, Patrick D. Noyes, Adam J. Voran, and R. P. Walsh

***Abstract*—In 2005, the Committee on Opportunities in High Magnetic Fields issued a challenge to develop a 30 T high-resolution NMR magnet. In response, the National High Magnetic Field Laboratory (NHMFL) is investigating all three commercially available high-temperature superconductors including REBCO, Bi-2212 and most recently, a reinforced Bi-2223 conductor supplied by Sumitomo Electric, designated Type HT-NX. Recent investigations of Type HT-NX conductor at the NHMFL and by others suggest that operation at hoop stress above 400 MPa, and total strain above 0.7% may be feasible. We have fabricated a test coil from a single 240 m length of HT-NX. The coil was successfully operated to 19.5 T in a 14 T background field, with a total applied strain of 0.8% and coil current density of 243 A/mm^2. The coil was cycled 20 times from half the design current to full current without observed degradation.**

***Index Terms*—Bi-2223, NMR magnets, layer-wound high-temperature superconductors (HTS) coils.**

I. Introduction

IN RESPONSE to the challenge in 2005 by the Committee on Opportunities in High Magnetic Fields (COHMAG) [1] to develop a 30 Tesla high-temperature superconducting (HTS) magnet for nuclear magnetic resonance (NMR) magnets, the National High Magnetic Field Laboratory (NHMFL) is investigating REBCO [2], Bi-2212 [3] and most recently, Sumitomo Type HT-NX Bi-2223 [4].

Sumitomo Type HT-NX conductor was introduced in 2015, and is composed of their standard Type H conductor with a high-strength nickel alloy lamination soldered under pre-tension to both sides. Findings from early tests [5] indicated that this conductor could be feasible for 30 Tesla class NMR magnets.

In 2016, Tohoku University, in partnership with Toshiba, built and tested a 25 Tesla cryogen free magnet using HT-NX conductor for the insert coil. The coil was made from stacked epoxy impregnated double-pancake modules. The coil made 11 Tesla with a current of 203 A [6].

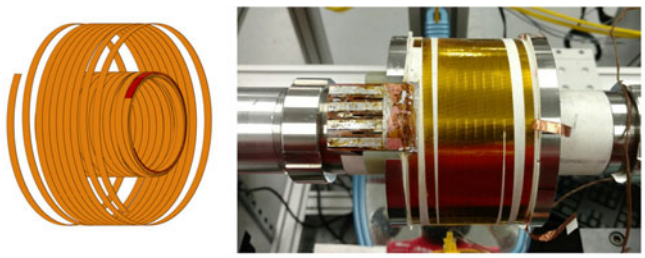

Fig. 1. CAD model rendering of test coil windings (left) and completed test coil on winding machine (right).

In 2015 Yanagisawa *et al.* at RIKEN tested a small layer wound paraffin impregnated coil using HT-NX conductor in a 17 T background field. The coil operated without degradation to 450 A, and showed permanent degradation after charging to 480–500 A [7].

In 2016, the NHMFL launched a program of fabrication and testing of layer-wound coils made with Type HT-NX conductor [8]. A series of test coils were designed to evaluate the performance of this conductor in conditions analogous to those expected in a 30 T NMR insert coil. A discussion of the design of the first coil is given, and results from testing to its design limits are reported.

II. Coil Technologies

A. Continuous Layer Winding

For high field homogeneity required for nuclear magnetic resonance (NMR) magnets, layer winding is preferred over stacked single- or double-pancake coil designs. The high aspect ratio of the Sumitomo Type HT-NX conductor cross section is challenging for a layer-wound coil, as the conductor must bend in the 'hard' direction to reverse the pitch of the winding in the transition from the previous layer to the next.

The NHMFL developed a method to minimize the added strain from bending in the hard direction at the layer transition. Each coil layer is parametrically modeled in CAD. Mechanical supports for the layer transitions and instructions to a computer-controlled coil winding machine are created from the model. Precise control of the placement of the HTS tapes in the coil winding pack is achieved. Features such as the layer transitions or splices are placed to avoid interfering with neighbor

Manuscript received August 29, 2017; accepted January 26, 2018. Date of publication February 2, 2018; date of current version March 9, 2018. This work was supported in part by the National Science Foundation (Grant DMR-1157490), in part by the State of Florida, and in part by the National Institute of General Medical Sciences of the National Institutes of Health under Grant R21GM111302. *(Corresponding author: William Scott Marshall.)*

W. S. Marshall is with the National High Magnetic Field Laboratory, Tallahassee, FL 32310 USA (e-mail: wsmarshall@magnet.fsu.edu).

M. D. Bird, D. C. Larbalestier, D. McRae, P. D. Noyes, A. Voran, and R. P. Walsh are with the National High Magnetic Field Laboratory, Tallahassee, FL 32310 USA.

Color versions of one or more of the figures in this paper are available online at http://ieeexplore.ieee.org.

Digital Object Identifier 10.1109/TASC.2018.2801296

TABLE I
TEST COIL DESIGN

Parameter	Value
Inner radius (a_1)	25 mm
Outer radius (a_2)	54 mm
Winding length (2b)	61 mm
Layers	88
Turns per layer	11
Current	450 A
Background field	14.1 T
Insert field	5.6 T
Inductance	42 mH
Coil constant	12.4 mT/A
Conductor length	240 m

TABLE II
SUMITOMO TYPE HT-NX CONDUCTOR PROPERTIES

Parameter	Value
Bare conductor width	4.5 mm
Bare conductor thickness	0.26 mm
Insulated conductor width	4.6 mm
Insulated conductor thickness	0.31 mm
Insulation thickness	0.013 mm × 4 layers
Critical current at self-field, 77 K	190 A
Tensile secant modulus	92 GPa
Critical tensile stress (>95% Ic retention)	480 MPa
Critical tensile strain	0.5%
Piece length	300 m

conductor turns, so excess radial buildup of the winding pack at the coil ends is avoided. Fig. 1 shows a CAD model and completed windings of the first test coil.

B. Terminals and Coil Support Structure

The terminals and coil support structure designs have evolved from prior work by the NHMFL for the 900 MHz NMR magnet [9] and the 32 T all-superconducting magnet [10]. The terminals are joined mechanically to the windings and the end flanges. The end flange connections allow the terminals to move with the windings to prevent the conductor from straining excessively.

The coil end flanges are axially compressed to the winding pack by arrays of preloaded Belleville springs, in a construction similar to the 32 T magnet [10]. The end flanges remain in contact with the winding pack as the coil displaces axially during cooldown and axial Lorentz loads during operation.

III. TEST COIL DESIGN

The radial dimensions of this coil were selected to be identical to a proposed coil making 7 T for a high-field NMR demonstration at 23 T [8]. The coil length was selected to enable use of a single conductor piece. The resulting coil design will demonstrate the performance of the conductor and coil technologies described in the previous section. The coil will demonstrate operation at a total strain limit of 0.8%.

Design parameters for the test coil are given in Table I. Conductor dimensions and parameters for the conductor, as received, are given in Table II.

The total stress and strain on the conductor in the coil windings are caused by winding tension, bending around the coil former, bending to reverse the winding pitch at the layer transition, differential thermal contraction between the coil former and conductor, and magnetic hoop stress. For these coils, winding tension is negligibly small, and the coil former material contracts at roughly the same rate as the conductor, and therefore can also be neglected. The equations used to compute stress and strain are given below.

Total strain on the conductor at any location in the winding pack is given by

$$\epsilon_{\text{wind}}(R) + \epsilon_{\text{hoop}}(R) = \epsilon_{\text{total}}(R) \tag{1}$$

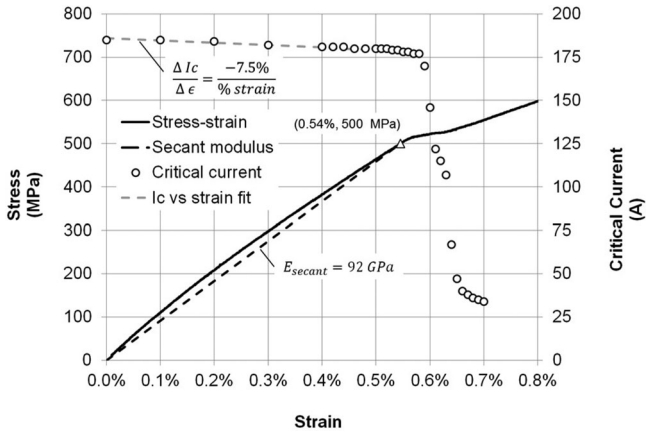

Fig. 2. Stress and critical current vs. strain, from [5]. Shown on this graph are reversible degradation in critical current vs. strain and secant modulus.

Where:

$$\epsilon_{\text{wind}}(R) = \frac{t_{\text{conductor}}}{2R} + \frac{w_{\text{conductor}}}{2C(R)} \tag{2}$$

$$\epsilon_{\text{hoop}}(R, z) = \frac{B(R, z) \cdot J_{\text{conductor}} \cdot R}{E_{\text{secant,conductor}}} \tag{3}$$

Where:

ϵ_{wind} is the winding strain
ϵ_{hoop} is the hoop strain
$t_{\text{conductor}}$ is the thickness of the bare conductor
$w_{\text{conductor}}$ is the width of the bare conductor
R is the winding radius
$C(R)$ is the radius of curvature of the conductor bend in the 'hard' direction at the layer transition
$J_{\text{conductor}}$ is the conductor current density, defined as the coil current divided by the area cross section of the bare conductor.
$E_{\text{secant, conductor}}$ is the secant modulus of the conductor, as defined in Fig. 2.

Magnetic compressive stress is:

$$\sigma_z = \frac{F_{\text{axial}}}{\pi\left({a_2}^2 - {a_1}^2\right)} \tag{4}$$

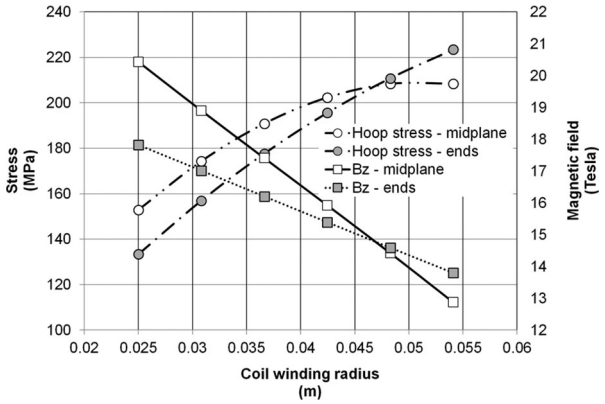

Fig. 3. Hoop stress and magnetic field at coil midplane and ends.

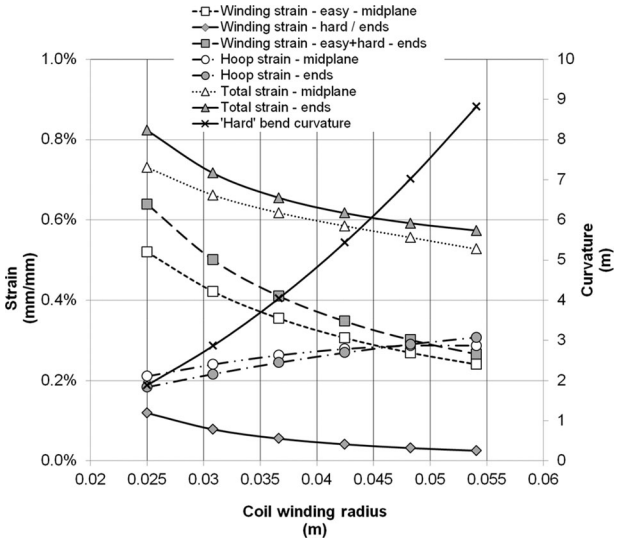

Fig. 4. Winding strain, hoop strain, total strain, 'hard' ben d curvature and strain vs. coil radius.

where F_{axial} is the force of two coil halves acting on one another at the coil midplane, and $\pi({a_2}^2 - {a_1}^2)$ is the area of the coil cross section normal to its axis.

The magnetic field and hoop stress at the coil midplane and ends is shown in Fig. 3.

Fig. 4 shows the winding, hoop and total strain at the coil midplane and ends. The location of maximum winding strain is at the innermost layer. The location of the maximum hoop strain is at the outermost layer. The magnitude of the strain contributions is such that the maximum total strain is dominated by the winding strain, and occurs on the inner diameter at the coil ends. The 'hard' direction bend adds 0.12% to the winding strain at the innermost layer.

In Fig. 5, the radial and axial field at the coil ends, the axial field at the coil midplane, and the critical currents at the coil midplane and ends are plotted vs. coil winding radius. The limiting magnetic field acts on the inner turn at the coil midplane. The radial component of field at the coil ends does not limit the critical current for this coil.

The integrated axial force acting on the coil midplane is 55 kN, for a maximum axial compressive stress of 8 MPa.

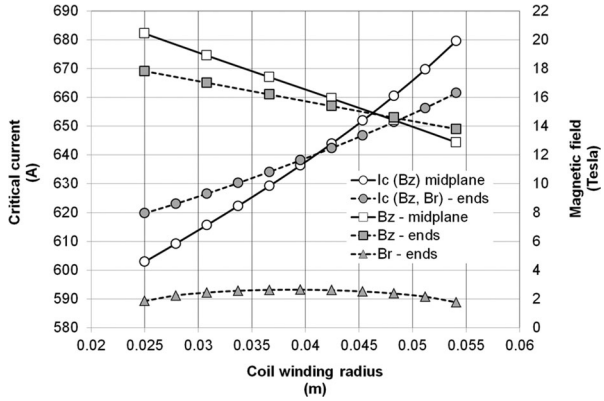

Fig. 5. Critical current and magnetic field vs. winding radius at midplane and coil ends.

TABLE III
SUMMARY OF TEST RESULTS

Parameter	Value
Central field	19.7 T
Field on windings	20.4 T
Number of load cycles	20
Maximum winding strain (1)	0.66%
Maximum hoop stress (2)	223 MPa
Maximum hoop strain (2)	0.31%
Maximum total strain (1)	0.82%
Current	450 A
Load cycles (225–450 A)	20
Critical current	588 A
Coil current density	243 A/mm^2
Conductor current density	299 A/mm^2
Coil inductance	42 mH
Coil resistance	8 $\mu\Omega$

(1) At coil ends, inner radius.
(2) At coil ends, outer radius.

IV. TEST RESULTS

The coil was operated in an LTS magnet in a background field of 14.1 Tesla. Results are summarized in Table III. After initially ramping the coil to 450 A, with holds at intermediate currents, the coil was cycled from 225–450 A for a total of 20 times at a rate of 0.6 A/s. A time history is shown in Fig. 6. Fig. 7 shows the measured and calculated field vs. current, with magnetization effects causing a small deviation from the calculated field. Fig. 8 plots the difference between the calculated and measured field contribution from the HT-NX coil. In this plot the coil magnetization is evident, with an added field of 0.2 Tesla at full current. Saturation is observed after eight charge/discharge cycles.

V. DISCUSSION OF RESULTS

For this coil, the dominant contributor to strain on the conductor is from winding. Bending in the 'easy' direction around the coil form and in the 'hard' direction to reverse the winding pitch both contribute. In this pre-strained condition, the coil was successfully operated to a total calculated strain of 0.82%, for 20 load cycles. The critical current of the coil is calculated to

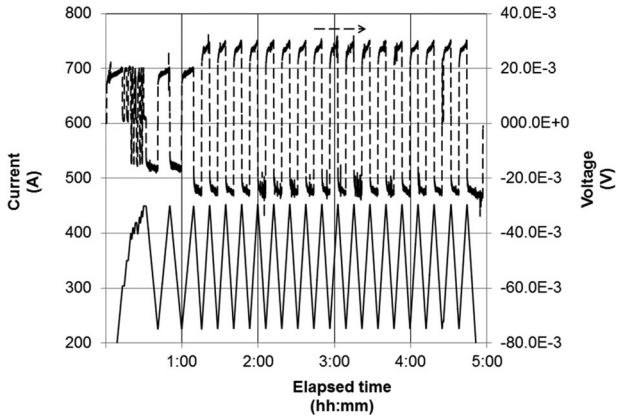

Fig. 6. Coil voltage and current vs. elapsed time.

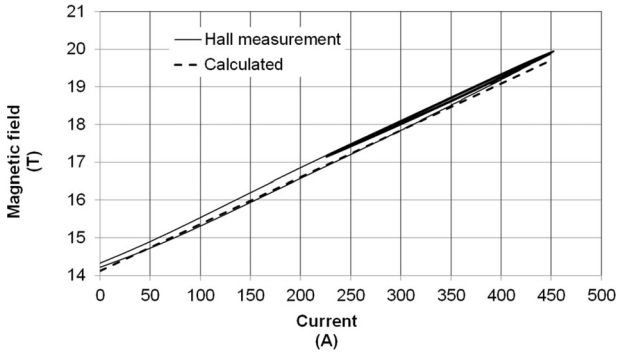

Fig. 7. Magnetic field vs. current.

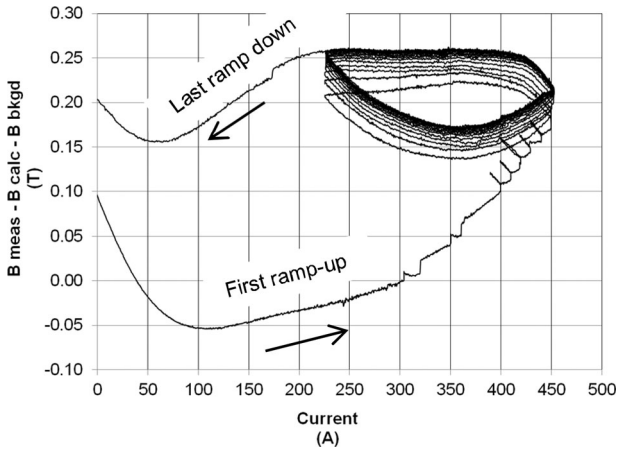

Fig. 8. Difference between calculated and measured field contribution from HT-NX coil.

be 588 A. At this current, the strain on the coil would be 0.9%, and damage to the superconductor would likely have occurred.

In Table II, and Fig. 2, the critical strain for HT-NX in pure tension is ∼0.5%. In a coil winding, the strain from bending and hoop loads is highest on the outer surface, and strain distribution through the conductor is non-uniform. The strain on the filaments is lower because they are closer to the neutral axis, and possibly because the silver matrix surrounding the filaments is plastically deforming. Previous work on small test articles [4], [5] has shown that HT-NX conductor can remain fully superconducting with strain in bending and hoop to ∼1%.

The two other known examples of coils made with HT-NX conductor [6], [7] do not explicitly report the total strain. Calculations from their published data however, indicate a maximum total strain of 0.7% for the RIKEN test coil, and 0.6% for the Tohoku insert coil.

VI. Conclusion

A coil, made from a 240 m length of Sumitomo Type HT-NX conductor, was wound and tested using fabrication technologies unique to the National High Magnetic Field Laboratory. The coil operated at an unprecedented peak total strain of 0.82%, surviving 20 load cycles. A careful accounting of the significant contributors to strain reveals that the bending in the 'hard' direction at the layer transitions is especially important for smaller diameter coils. This suggests that there may be a practical minimum inner diameter for these conductors. This result informs an ongoing discussion about practical design limits for high field magnets made from this conductor.

Acknowledgment

The authors are grateful for the skilled and focused work of E. Arroyo and B. Sheppard of the National High Magnetic Field Laboratory to fabricate and test the coils. The authors would also like to thank R. Shaw at Sumitomo Electric for his responsiveness and support of our effort.

References

[1] P. B. Moore *et al.*, *Opportunities in High Magnetic Field Science*, Washington, DC, USA: The National Academies Press, 2005. [Online]. Available: http://www.nap.edu/catalogue/11211.html

[2] H. W. Weijers *et al.*, "Progress in the development and construction of a 32-T superconducting magnet," *IEEE Trans. Appl. Supercond.*, vol. 26, no. 4, Jun. 2016, Art no. 4300807.

[3] D. C. Larbalestier *et al.*, "Isotropic round-wire multifilament cuprate superconductor for generation of magnetic fields above 30 T," *Nature Mater.*, vol. 13, no. 4, pp. 375–381, 2014.

[4] A. Godeke *et al.*, "A feasibility study of high-strength Bi-2223 conductor for high-field solenoids," *Supercond. Sci. Technol.*, vol. 30, no. 3, Jan. 30, 2017.

[5] W. S. Marshall *et al.*, "Investigation of the strain limit of Sumitomo Type HT-NX conductor and its impact on high field coil design," presented at the 8th Workshop on Mechanical and Electromagnetic Properties of Composite Superconductors, Tallahassee, FL, USA, Mar. 2016.

[6] S. Hanai *et al.*, "Development of an 11 T BSCCO insert coil for a 25 T cryogen-free superconducting magnet," *IEEE Trans. Appl. Supercond.*, vol. 27, no. 4, Jun. 2017, Art. no. 4602406.

[7] Y. Yanagisawa *et al.*, "Combination of high hoop stress tolerance and a small screening current-induced field for an advanced Bi-2223 conductor coil at 4.2 K in an external field," *Supercond. Sci. Technol.*, vol. 28, no. 12, Oct. 23, 2015.

[8] W. S. Marshall *et al.*, "Bi-2223 test coils for high resolution NMR magnets," *IEEE Trans. Appl. Supercond.*, vol. 27, no. 4, Jun. 2017, Art. no. 4300905.

[9] W. D. Markiewicz *et al.*, "Method of manufacturing a superconducting magnet," U.S. Patent 6 735 848, May 18, 2004.

[10] A. Voran *et al.*, "Design and testing of terminals of REBCO Coils for 32 T all-superconducting magnet," *IEEE Trans. Appl. Supercond.*, vol. 24, no. 3, Jun. 2014, Art. no. 4601204.

[11] A. Voran *et al.*, "Mechanical support of the NHMFL 32 T superconducting magnet," *IEEE Trans. Appl. Supercond.*, vol. 27, no. 4, Jun. 2017, Art. no. 4300305.